Proc. Natl. Acad. Sci. USA
Vol. 92, pp. 4962–4966, May 1995
Biophysics

Experimental evidence for hydrogen-bonded network proton transfer in bacteriorhodopsin shown by Fourier-transform infrared spectroscopy using azide as catalyst

JOHANNES LE COUTRE*, JORG TITTOR†, DIETER OESTERHELT†, AND KLAUS GERWERT*‡

*Lehrstuhl für Biophysik, Fakultät Biologie, Ruhr-Universität-Bochum 44780 Bochum, Federal Republic of Germany; †Max-Planck-Institut für Biochemie, Am Klopferspitz 18a, 82152 Martinsried, Federal Republic of Germany

Communicated by Manfred Eigen, Max-Planck-Institut für Biophysikalische Chemie, Göttingen, Federal Republic of Germany, January 18, 1995

ABSTRACT **Experimental evidence for proton transfer via a hydrogen-bonded network in a membrane protein is presented. Bacteriorhodopsin's proton transfer mechanism on the proton uptake pathway between Asp-96 and the Schiff base in the M-to-N transition was determined. The slowdown of this transfer by removal of the proton donor in the Asp-96 → Asn mutant can be accelerated again by addition of small weak acid anions such as azide. Fourier-transform infrared experiments show in the Asp-96 → Asn mutant a transient protonation of azide bound to the protein in the M-to-N transition and, due to the addition of azide, restoration of the IR continuum band changes as seen in wild-type bR during proton pumping. The continuum band changes indicate fast proton transfer on the uptake pathway in a hydrogen-bonded network for wild-type bR and the Asp-96 → Asn mutant with azide. Since azide is able to catalyze proton transfer steps also in several kinetically defective bR mutants and in other membrane proteins, our finding might point to a general element of proton transfer mechanisms in proteins.**

The retinal protein bacteriorhodopsin (bR), probably the best understood example of an ion pump, is a suitable system to study intramolecular proton transfer in proteins (1). Crucial events for the transport mechanism during the photocycle via the intermediates J, K, L, M, N, and O are the light-induced isomerization of all-*trans*-retinal to 13-*cis*-retinal in the BR-to-J photoreaction (where BR is the ground state of the bR molecule), the deprotonation of the Schiff base which is the binding site between chromophore and protein, (2–4), and protonation changes of internal aspartic acids (5). Fourier-transform infrared (FTIR) spectroscopy of mutant bRs identified the proton acceptor on the proton release pathway as Asp-85 (D85) (6–8) and the proton donor on the proton uptake pathway as D96 (8). The proton acceptor D85 is protonated in the L-to-M reaction, in which the Schiff base becomes deprotonated, whereas the donor D96 is deprotonated in the M-to-N transition, in which the Schiff base is reprotonated (9). Evidence for the catalytic role of these aspartic acids is contributed by electrical charge displacement measurements showing disturbed proton transport in D85X and D96X mutants (10, 11). These results on the reaction mechanism were strongly confirmed in all details in a series of succeeding publications (for review, see ref. 12). The atomic structural model of bR as developed from high-resolution electron microscopic studies proposed the positions of D85 and D96 on either side of the retinal (13). Therefore they are correctly located for their role in the vectorial proton translocation process.

However, the donor, D96, is positioned in the structural model about 12 Å from the acceptor, the Schiff base (13). Even though the resolution of the structure in the cross section of the molecule is only about 10 Å and does not predict the exact position of D85 and D96, they belong to the same α helix, C, and at least one of them must have, independent of the model, a distance from the Schiff base which is too far for direct proton transfer. The time-resolved FTIR experiments suggest at first glance a closer distance because deprotonation of D96 and reprotonation of the Schiff base are described by the same apparent rate constant (9). Nevertheless, fast and kinetically unresolved proton transfer via intermediary donor and acceptor groups in the M-to-N reaction could explain the 12-Å distance between donor D96 and acceptor Schiff base (8). Analysis of the "azide effect" at the atomic level might contribute to the elucidation of the proton transfer mechanism between D96 and the Schiff base. Azide and other anions of small weak acids are shown to repair the kinetic defect in the M decay of the D96N mutant, which is caused by the lack of the donor (14–16). Further studies have revealed that azide not only accelerates reprotonation but also deprotonation steps in other mutants of bR (17). Besides bR, azide also accelerates proton transfer reactions in other proteins—e.g., in the anion pump halorhodopsin (18) and in photosynthetic reaction centers (19). These observations point to a more general catalytic influence on proton transfer reactions in proteins.

We performed time-resolved FTIR experiments to analyze how azide accelerates the M-to-N transition in D96N. A molecular model of the action of azide and its implication for the proton transfer mechanism in wild-type bR is suggested and discussed.§

MATERIALS AND METHODS

Purple membranes from wild-type and mutant *Halobacterium salinarium* were prepared by the standard protocol (20). IR samples were prepared by using protein pellets. This guarantees maintenance of the preadjusted pH value, the azide concentration, and sufficient hydration of the sample. Typically, 1 ml of suspension with a final protein concentration of 2 mg/ml was used. Azide and phosphate buffer were adjusted to 100 mM at pH 5 and the suspension was centrifuged at 50,000 × *g* for 4 hr. The pellet was squeezed between two IR windows separated by a 2.5-μm Mylar spacer, resulting in a protein concentration of about 30 mM. As a control, flash-induced absorbance changes in the visible spectral region demonstrated that azide acts in hydrated films required for FTIR spectroscopy as in suspension. Samples for time-resolved experiments were prepared at pH 5 because IR bands of azide or hydrogen azide can best be detected at a pH close to the pK_a of azide (pK_a = 4.7). The FTIR measurements were per-

The publication costs of this article were defrayed in part by page charge payment. This article must therefore be hereby marked "*advertisement*" in accordance with 18 U.S.C. §1734 solely to indicate this fact.

Abbreviations: bR, bacteriorhodopsin; BR, ground state of the bR molecule; FTIR, Fourier-transform infrared.

‡To whom reprint requests should be addressed.

§The essential part of this work was presented at the Sixth International Conference on Retinal Proteins, June 19–24, 1994, Leiden, Netherlands.

formed on a modified Bruker (Billerica, CA) IFS 88 spectrometer using static techniques and the time-resolved fast-scan technique (21). Each measurement was done at least twice. To detect the complete M decay with the fast-scan technique, the samples were cooled to 263 K. For the static measurements a total of 40,000 scans were averaged. Data were taken in blocks of 100 scans each to control the baseline during the measurement. In the static measurements excitation with actinic light was done with a 100-W halogen lamp and an OG515 cutoff filter. Time-resolved fast-scan measurements were performed and analyzed with a global-fit method (22, 23).

RESULTS

Protonation Changes of Azide During Accelerated Proton Transfer in bR. In D96N as compared with the wild-type protein, removal of the internal proton donor D96 not only slows down M decay but also M formation. Addition of azide to the D96N mutant results in even faster M formation and decay than in the wild-type protein and in a kinetic separation of M decay and bR recovery (data not shown) (14–17, 24, 25). Furthermore, azide also accelerates M formation and decay in the wild-type protein about 2-fold (data not shown). We conclude that azide can substitute for the catalytic role of D96 in the proton transport function of bR and has a slight catalytic effect on the molecule even in wild-type bR.

To elucidate the molecular mechanism of this catalytic effect, the possible protonation changes of azide during the photocycle were determined. The protonation state of azide in the various intermediates can be analyzed by its absorbance changes in the IR spectral region (26, 27). In addition, the IR frequencies of azide and hydrogen azide are sensitive to the protic character and to the polarity of the environment. The azide and hydrogen azide absorption bands are well separated, by about 100 cm^{-1}. Increasing hydrophobicity shifts the frequencies of the azide band from 2050 cm^{-1} in water down to 2018 cm^{-1} in dimethyl sulfoxide and the hydrogen azide bands from 2148 cm^{-1} in water to 2129 cm^{-1} in dimethyl sulfoxide (28).

During bR's photocycle an azide band at 2040 cm^{-1} disappears and a hydrogen azide band at 2132 cm^{-1} appears, indicating transient protonation of azide (Fig. 1*A*) (25). With the dependence presented in ref. 28, the frequencies of the two bands indicate protonation of azide in the hydrophobic interior of the protein rather than protonation in the aqueous bulk phase. The size of the absorbance changes as compared with the background absorbance of azide/hydrogen azide added to the sample suggests transient protonation of about one azide molecule per bR under the conditions applied.

The time dependence of disappearance of the azide band at 2040 cm^{-1} and of appearance of the hydrogen azide band at 2132 cm^{-1} allows the identification of the photocycle intermediate in which azide becomes protonated (Fig. 1*A*). The absorbance changes at 410 nm reflect M formation and the change at 1186 cm^{-1} represents Schiff base reprotonation in the M-to-N transition. Comparison of the traces in Fig. 1*A* and *B* indicates transient protonation of azide after M formation, during the lifetime of the N intermediate. Both the disappearance of the azide band and the appearance of the hydrogen azide band can be described by the apparent rate constant k_4 as revealed by global-fit analysis (for nomenclature see ref. 23). This rate constant describes mainly the M-to-N transition. Global-fit analysis of the light-induced absorbance changes of D96N with and without azide shows that the most affected apparent rate constant is k_4. The analysis yields an increase due to the addition of azide from τ_4 (= $1/k_4$) = 286 ms to τ_4 = 6 ms. The transient protonation of azide ceases with the decay of the N intermediate.

Internal Hydrogen-Bonded Network. To elaborate differences between the intramolecular reactions during N rise and decay in D96N with and without azide, the respective amplitude spectra of the rate constants were compared. The amplitude spectra of k_4 reflect the protein reactions mainly during the M-to-N transition, whereas the k_6 amplitude spectra mainly represent the N decay reaction. The respective amplitude spectra of k_4 and k_6 with and without azide agree within the experimental error. The signal/noise ratio is much better for the amplitude spectra of the rate constant k_6, making them more appropriate for a comparison (Fig. 2). Since no deviations in the amplitude spectra of N rise and decay rate

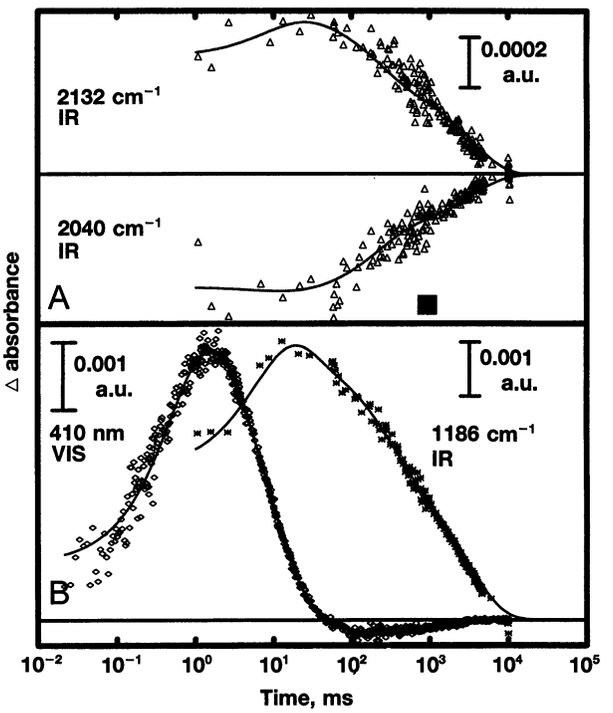

FIG. 1. Comparison of selected absorption changes in the visible and IR spectral range. (*A*) Formation of hydrogen azide can be followed at 2132 cm^{-1}, and the corresponding decrease of azide at 2040 cm^{-1}. (*B*) The absorbance change at 410 nm monitor formation and decay of the M intermediate. The absorbance change at 1186 cm^{-1} indicates protonation of the Schiff base in a 13-*cis* configuration (N intermediate). a.u., Absorbance unit.

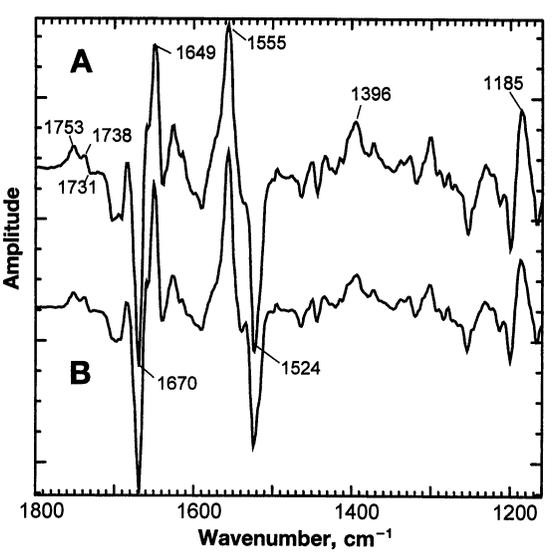

FIG. 2. IR amplitude spectra of the rate constant (k_6) describing the N-to-BR transition. (*A*) D96N without azide; τ_6 (= $1/k_6$) = 3100 ms. (*B*) D96N with azide; τ_6 = 2200 ms.

constants are identified, no indication for additional protonation changes of protein side groups in the presence of azide is found.

The question then arises of which group donates the proton to azide. IR continuum band changes are observed during the bR photocycle (9). Such continuum bands are indicative of hydrogen-bonded networks as shown for several model compounds (29). An appearance of a small continuum band between 2300 and 1800 cm^{-1} is observed in the BR − L difference spectrum measured with the static technique, in agreement with ref. 29. In the BR − N difference spectrum the disappearance of a small continuum band is seen (9). Great care was taken to exclude baseline drifts, which in principle could cause similar effects in the difference spectra. Due to limited space the data are not shown here. Fortunately, in contrast to the static technique the time-resolved fast-scan technique allows measurements without baseline drifts in the desired time range (21). This technique is more appropriate to analyze changes in the small continuum bands. Even though the absorbance change at a single wavenumber is small, global-fit analysis still allows a reliable determination of the continuum bands time course because a broad spectral range is analyzed simultaneously (22, 23). The analysis shows, in agreement with static measurements, that in wild-type bR a small continuum band appears with the L intermediate and disappears below the level of the initial state in the N intermediate. As a typical example out of this broad continuum band, the absorbance change at 1900 cm^{-1} is presented in Fig. 3*A*, which shows appearance of a continuum band in L, subsequent decrease in the L-to-M transition, and disappearance of a continuum band in N. In the mutant protein, in contrast to wild-type bR, no disappearance of a continuum band in the N intermediate is observed (compare Fig. 3 *A* and B). But again a disappearing continuum band as in wild-type bR is detected in N when azide is added to the mutant (Fig. 3*C*). For illustration of the entire continuum band, the absorbance changes between 2300 and 1800 cm^{-1} of D96N plus azide are shown in a three-dimensional graph (Fig. 4). Besides the disappearing azide band at 2040 cm^{-1} and the appearing hydrogen azide band at 2132 cm^{-1}, a broad small positive band present in L disappears with N (compare for the kinetics Fig. 3*C*). In summary, addition of azide to D96N leads to restoration of IR continuum band changes identical to those in wild-type bR.

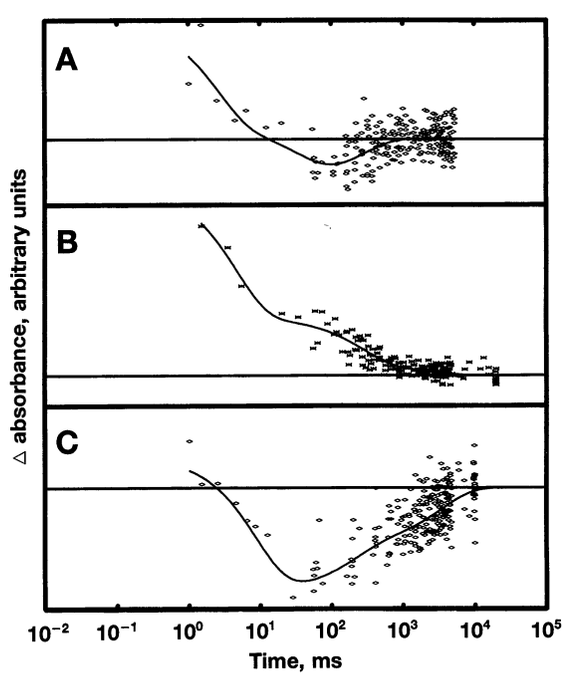

FIG. 3. Absorption changes at 1900 cm^{-1} at pH 5 and 263 K for wild-type bR (*A*), D96N (*B*) and D96N with azide (*C*). The amplitude of the absorption change in *C* normalized to the band at 1755 cm^{-1} is about twice that in *A*.

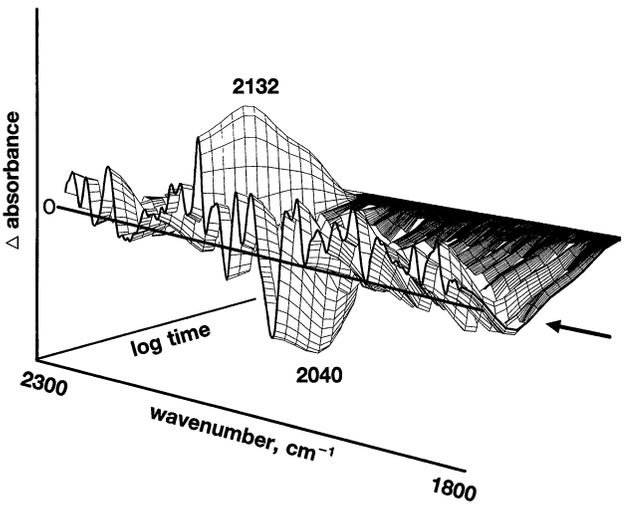

FIG. 4. Three-dimensional graph of the absorbance changes between 2300 cm^{-1} and 1800 cm^{-1} in the time range from 1 ms to 1.5 s for D96N with azide at pH 5 and 263 K. The arrow points to the minimum of the broad continuum band in N.

Location of Azide. To locate azide within the protein's topography the sensitivity of the azide absorption frequency to its environment is used (28). We expect that mutation of a protein side group located near azide would shift the frequency of its absorption band. In Fig. 5 the disappearing azide and appearing hydrogen azide bands in different mutants are shown. Only mutations at position 85 shift the azide band in the bR ground state, but not the mutation of D115, R82, or D96. The hydrogen azide band in the intermediate states is not shifted in any of these mutants.

DISCUSSION

Addition of azide to D96N and to wild-type bR accelerates M rise and decay. Mainly the M-to-N transition described by the apparent rate contant k_4 is accelerated by azide.

The IR absorbance changes indicate a transient protonation of about one azide per bR during the M-to-N transition in the

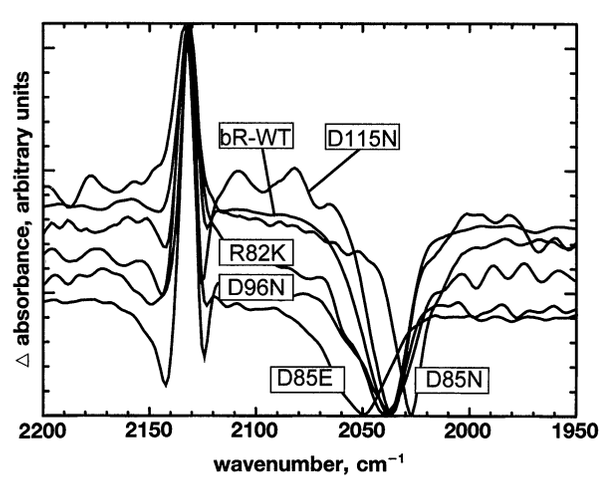

FIG. 5. Difference spectra obtained under continuous illumination of wild-type bR (bR-WT), D96N, D115N, R82K, D85N, and D85E at pH 5 and 258 K in the presence of azide. Only an amino acid exchange at position 85 shifts the azide band.

D96N mutant and in the wild type. The results rule out the earlier suggestions that hydrogen azide substitutes for D96 as internal proton donor (14–16). Mutation of D96 does not shift the azide absorption frequency as compared with wild-type bR, but mutation of D85 does. This frequency shift is characteristic for a change in the azide environment. Therefore binding of azide close to D96 seems more unlikely than binding closer to D85 in the proton release pathway. The amplitude spectra of the N intermediate with and without azide show no differences, excluding different intramolecular protein reactions in the two samples. This rises the questions of how azide accelerates the photocycle and from where it is protonated.

The only spectral differences found between samples with and without azide are changes in the IR continuum band. In contrast to wild-type bR no continuum band disappears in D96N during the retarded M-to-N transition. Addition of azide accelerates the M-to-N transition and a disappearing continuum band is observed again as in wild-type bR. In a series of experiments Zundel and coworkers demonstrated that delocalized protons in a hydrogen-bonded network caused broad IR continuum bands (29). Increase of the IR continuum absorption indicates stronger delocalization of at least one proton into the network (higher proton polarizability) and a decrease indicates less delocalization (lower proton polarizability). The changes in the IR continuum band during the photocycle indicate the existence of an internal hydrogen-bonded network in bR which undergoes proton polarizability changes during the photocycle. Since addition of azide to D96N restores the wild-type bR infrared continuum band changes, we propose an influence of azide on the arrangement of the intramolecular hydrogen-bonded network.

Our conclusions are summarized in a model in Fig. 6.

In the initial BR ground state of D96N, azide is proposed to be located close to D85. Even if positioning of an additional negative charge close to D85 and D212 seems unlikely, a H_3O^+, for example, might counterbalance the negative charge. Nevertheless, molecular dynamics calculations, taking into account the electrostatic interactions, predict that azide can actually be positioned in the extracellular pathway but not close to D96 in the hydrophobic region of the cytoplasmic pathway (M. Engels, J.l.C., and K.G., unpublished data). In agreement with this proposal, azide affects the pK_a of the purple-to-blue transition in which D85 becomes protonated from the bulk (data not shown).

An internal hydrogen-bonded network between D96 in wild-type bR or N96 in mutant bR and the Schiff base could explain the observation of continuum band changes during proton pumping. Such a hydrogen-bonded network enables fast proton transfer (30–33). Addition of a proton at one end of the network induces hopping of protons from the donors to the acceptors, resulting in almost simultaneous proton release at the other end [see Fig. 6, network in M (I)]. Proton transfer leads within the network to a defect which has to be restored by rotation in a second step to regenerate the initial conformation [see Fig. 6, network in N (II)]. Internal water, protein side groups, and the backbone might contribute hydrogen-bonds to such a network. There is experimental evidence for internal bound water in bR (34–37). Molecular dynamics calculations on the bR structural model proposed by Henderson *et al.* (13) orient a chain of water molecules just between D96 and the Schiff base as presented in the scheme (38, 39).

In the intermediate L after light-induced 13-*cis* isomerization of retinal and pK reduction of the protonated Schiff base an increase of proton polarizibility is observed, meaning that the proton is partially located at the acceptor D85. Partial protonation of D85 is indicated by a small absorption increase at 1763 cm^{-1} already in L (see figure 1 in ref 8). The 1763-cm^{-1} band indicates the protonation state of D85 and is fully developed, meaning fully protonated, in M. Furthermore, D96 undergoes an environmental change in L, concluded from the frequency shift from 1748 cm^{-1} to 1752 cm^{-1} (see figure 1 in ref. 8). This change of the chemical microenvironment of D96 already in L points to a connection between the proton release and proton uptake pathway. Addition of azide increases the

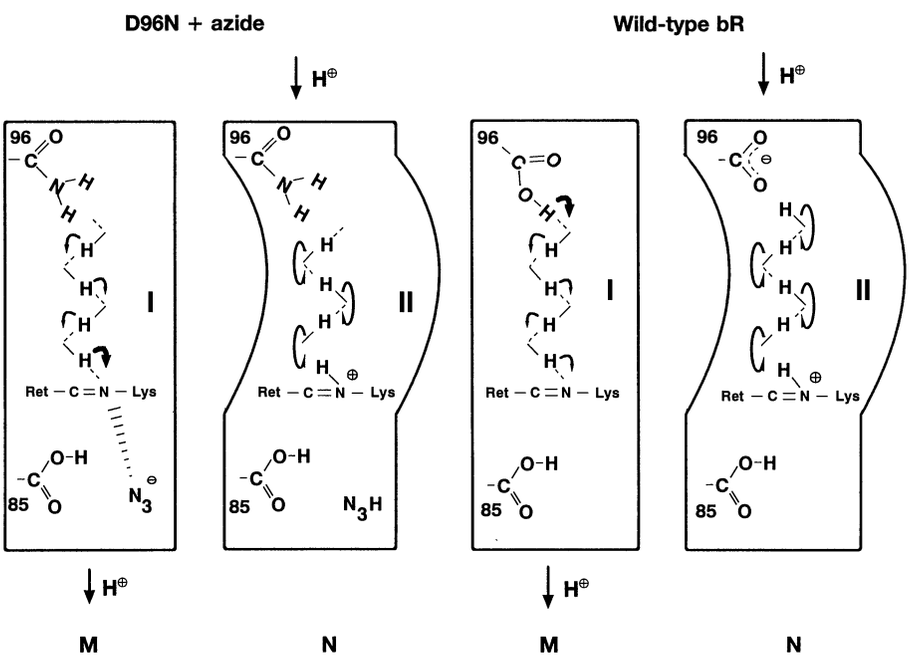

FIG. 6. Schematic model of the catalytic mechanism of azide during the D96N photocycle (see also *Discussion*). In the M-to-N transition, azide affects, as defect proton, the orientation of a hydrogen-bonded network in the proton uptake pathway, which is indicated with stripes. This results in a fast proton uptake reaction of the Schiff base (I). The net difference of two charges between M and N in D96N + azide is due to delocalized charges in the network, which become localized at the Schiff base and azide in N. The change of backbone hydrogen bonds might contribute to the hydrogen-bonded network, indicated as a conformational change of the protein in N. Also, single water molecules might contribute to the network. In wild-type bR the proton of D96 is donated to the upper side of the hydrogen-bonded network, resulting at the lower side in fast reprotonation of the Schiff base. A rotational step (II) during the N-to-bR recovery is required to restore the proton "wire" to the original state.

negative charge density in the proton release pathway in D96N and wild-type bR. This increase could facilitate the proton movement to D85, explaining the acceleration of the L-to-M transition in mutant and wild-type bR.

During the M-to-N transition in the wild-type protein, D96 is proposed to donate its proton to one end of the hydrogen-bonded network, which then releases on the other end a proton almost simultaneously to reprotonate the Schiff base (see Fig. 6). The IR continuum band disappears in N in wild-type bR and D96N in the presence of azide. The disappearance indicates a less delocalized proton. D96 is deprotonated only in N, and therefore its proton cannot be delocalized into the network in this state. Hydrogen-bond changes of backbone carbonyl groups in the M-to-N transition might contribute to establish the proton transfer network. This backbone movement, symbolized in Fig. 6 by a structural deformation in N, seems to be the rate-limiting step because proton transfer reactions across such a hydrogen-bonded network are usually faster than the 1-ms M-to-N transition (30).

D96N, in contrast to wild-type bR, has no protonable side group which could contribute an additional proton to the upper side of the network, and therefore the reprotonation of the Schiff base is slowed down. Two alternative mechanisms are proposed for how azide can accelerate this step on the basis that azide is assumed to be located in the proton release pathway close to position 85. (*i*) The hydrogen-bonded network might have on its lower side connections to both the Schiff base and azide. In the scheme only a linear network is drawn; in reality, the network might span three dimensions. In this case azide works as an additional defect proton on the lower network side, thereby inducing proton transfer in the same direction as an additional proton from D96 on the upper side in wild-type bR. (*ii*) Azide influences allosterically the correct arrangement of a network between D96 and the Schiff base. Since the Schiff base has lost its positive charge in M, azide as an anion can induce electrostatically the proper network alignment, which is also supported by the backbone movement in the M-to-N transition. The Schiff base lone pair of electrons might be repulsed away from the negative azide anion toward the hydrogen-bonded network.

The upper side of the network is reprotonated from the cytoplasmic external medium. The two mechanisms are in agreement with the effect of azide on the parameters of proton transfer. The lack of D96 slows the reprotonation of the Schiff base not by an increase in the enthalpy change of activation but by a decrease in the entropy change of activation. This suggests that azide reduces the multitude of reprotonation pathways to the Schiff base in D96N to one preferential pathway (14, 40).

In N also does azide become protonated in addition to the Schiff base. The azide proton seems not to be donated by the protein itself, because the N amplitude spectra give no indication for additional protonation changes of protein groups due to the addition of azide (Fig. 2). The proton therefore might be donated by the bulk phase or internal H_2O/H_3O^+, which could be connected to the network. The continuum band disappearance normalized to the respective band at 1755 cm^{-1}, which indicates D85 protonation in N, shows about twice the amplitude in D96N with azide as in wild-type bR, in agreement with the proposal that the network releases a second proton in D96N in the presence of azide (see Fig. 3).

At pH 7.5, time-resolved measurements show only an environmental change of azide in the N time range instead of transient protonation as at pH 5.0, even though an azide effect on the photocycle kinetics is observed (28). Either at this pH hydrogen azide ($pK_a = 4.7$) equilibrates too fast with the bulk to be accumulated and detected, or no protonation of azide occurs at all. However, the results are in agreement with the proposed role of the azide to catalyze, as an anion, allosterically the transfer in the hydrogen-bonded network. Its protonation seems not to be necessary.

Direct experimental evidence for the long-proposed (30, 33) intramolecular protein proton transfer via a hydrogen-bonded network is given and seems to be a paradigm for several proteins.

We thank Prof. R. S. Goody for hospitality at the Max-Planck-Institut für Molekulare Physiologie in Dortmund. J.l.C. enjoys a fellowship from the Boehringer Ingelheim Fonde. K.G. acknowledges support by a grant of the Deutsche Forschungsgemeinschaft (Ge-599/7-1).

1. Oesterhelt, D. & Stoeckenius, W. (1973) *Proc. Natl. Acad. Sci. USA* **70,** 2853–2857.
2. Braiman, M. S. & Mathies, R. (1980) *Biochemistry* **11,** 5421–5428.
3. Lewis, A., Spoonhower, J., Bogomolni, R. A., Lozier, R. H. & Stoeckenius, W. (1974) *Proc. Natl. Acad. Sci. USA* **71,** 4462–4466.
4. Longstaff, C. & Rando, R. (1987) *Biochemistry* **26,** 6107–6113.
5. Engelhard, M., Gerwert, K., Hess, B., Kreutz, W. & Siebert, F. (1985) *Biochemistry* **24,** 400–407.
6. Braiman, M. S., Mogi, T., Marti, T., Stern, L. J., Khorana, H. G. & Rothschild, K. J. (1988) *Biochemistry* **27,** 8516–8520.
7. Fahmi, K., Weidlich, O., Engelhard, M., Tittor, J., Oesterhelt, D. & Siebert, F. (1992) *Photochem. Photobiol.* **56,** 1073–1083.
8. Gerwert, K., Hess, B., Soppa, J. & Oesterhelt, D. (1989) *Proc. Natl. Acad. Sci. USA* **86,** 4943–4947.
9. Gerwert, K., Souvignier, G. & Hess, B. (1990) *Proc. Natl. Acad. Sci. USA* **87,** 9774–9778.
10. Butt, H. J., Fendler, K., Bamberg, E., Tittor, J. & Oesterhelt, D. (1989) *EMBO J.* **8,** 1657–1663.
11. Holz, M., Drachev, L. A., Mogi, T., Otto, H., Kaulen, A. D., Heyn, M. P., Skulachev, V. P. & Khorana, H. G. (1989) *Proc. Natl. Acad. Sci. USA* **86,** 2167–2171.
12. Lanyi, J. (1993) *Biochim. Biophys. Acta* **1183,** 241–261.
13. Henderson, R., Baldwin, J. M., Ceska, T. A., Zemlin, F., Beckmann, E. & Downing, K. H. (1990) *J. Mol. Biol.* **213,** 899–929.
14. Tittor, J., Soell, C., Oesterhelt, D., Butt, H. J. & Bamberg, E. (1989) *EMBO J.* **8,** 3477–3482.
15. Otto, H., Marti, T., Holz, M., Mogi, T., Lindau, M., Khorana, H. G. & Heyn, M. P. (1989) *Proc. Natl. Acad. Sci. USA* **86,** 9228–9232.
16. Danshina, S. V., Drachev, L. A., Kaulen, A. D., Khorana, H. G., Marti, T., Mogi, T. & Skulachev, V. P. (1992) *Biokhimiya* **57,** 1574–1585.
17. Tittor, J., Wahl, M., Schweiger, U. & Oesterhelt, D. (1994) *Biochim. Biophys. Acta* **1187,** 191–197.
18. Hegemann, P., Oesterhelt, D. & Steiner M. (1985) *EMBO J.* **4,** 2347–2350.
19. Takahashi, E. & Wraight, C. A. (1991) *FEBS Lett.* **283,** 140–144.
20. Oesterhelt, D. & Stoeckenius, W. (1974) *Methods Enzymol.* **31,** 667–678.
21. Gerwert, K. (1993) *Curr. Opin. Struct. Biol.* **3,** 769–773.
22. Souvignier, G. & Gerwert, K. (1992) *Biophys. J.* **51,** 627–635.
23. Heßling, B., Souvignier, G. & Gerwert, K. (1993) *Biophys. J.* **65,** 1929–1941.
24. Drachev, L. A., Kaulen, A. D. & Komrakov, A. Y. (1994) *Biochemistry (Moscow)* **59,** 287–291.
25. le Coutre, J. & Gerwert, K. (1994) *Springer Proc. Phys.* **74,** 256–257.
26. Colthup, N. B., Daly, L. H. & Wiberly, S. E. (1990) *Introduction to Infrared and Raman Spectroscopy* (Academic, Orlando, FL), 3rd Ed., p. 243.
27. Dows, D. A. & Pimentel, G. C. (1955) *J. Chem. Phys.* **23,** 1258–1263.
28. le Coutre, J. & Gerwert, K. (1992) in *Structures and Functions of Retinal Proteins*, ed. Rigaud, J. L. (Libbey, Eurotext), vol. 221, pp. 127–130.
29. Zundel, G. (1992) *Trends Phys. Chem.* **3,** 129–156.
30. Eigen, M. & DeMaeyer, L. (1958) *Proc. Roy. Soc. London A* **247,** 505–533.
31. Nagle, J. F. & Tristram-Nagle, S. (1983) *J. Membr. Biol.* **74,** 1–14.
32. Brünger, A., Schulten, Z. & Schulten, K. (1983) *Z. Phys. Chem. (Munich)* **136,** 1–63.
33. Onsager, L. (1967) in *Neurosciences*, ed. Schmitt, F. O. (Rockefeller Univ. Press, New York), pp. 75–79.
34. Hildebrandt, P. & Stockburger, M. (1984) *Biochemistry* **19,** 5539–5548.
35. Papadopoulos, G., Dencher, N., Zaccai, G. & Büldt, G. (1990) *J. Mol. Biol.* **214,** 15–19.
36. Maeda, A., Sasaki, J., Yoshinori, S. & Yoshizawa, T. (1992) *Biochemistry* **31,** 462–467.
37. Heberle, J. & Dencher, N. A. (1990) *FEBS Lett.* **277,** 277–280.
38. Humphrey, W., Logunov, I., Schulten, K. & Sheves, M. (1994) *Biochemistry* **33,** 3668–3678.
39. Engels, M., Gerwert, K. & Bashford, D. (1995) *Biophys. Chem.*, in press.
40. Miller, A. & Oesterhelt, D. (1990) *Biochim. Biophys. Acta* **1020,** 57–64.